

# **Characterization of the Interaction Between Myosin XIa and RabA4 in *Physcomitrella patens***



**A Major Qualifying Project  
Submitted to the Faculty of  
WORCESTER POLYTECHNIC INSTITUTE  
in partial fulfillment of the requirements for the  
Degree of Bachelor of Science**

By:  
Erin Armstrong

Date: 26 April 2012

Report Submitted To:

Professor Luis Vidali  
Worcester Polytechnic Institute

## Abstract

In the moss *Physcomitrella patens*, myosin XI mediated polarized tip growth is essential for growth and expansion. It has been hypothesized that, during polarized growth, secretory vesicles move to the tip of the expanding cell via an interaction between the myosin XI globular tail and RabA4. In this study, we show that several mutations in the putative binding region for RabA4 on the myosin XI tail produce the same phenotype as a myosin XIa knockdown, suggesting an interaction with RabA4.

## Acknowledgements

I would like to first thank my advisor, Dr. Luis Vidali for all of his help and support throughout the duration of my project. Moreover, I would like to thank Fabienne Furt for all of her helpful guidance and advice over the course the year. Next, I would like to extend my thanks to all of the other members of the Vidali lab: Yen-Chun Liu, Zhiyuan Shen, Robert Collatos and Jeffrey Bibeau. Finally, thank you to Dr. Kaye Peterman, the Gateway Staff and everyone at WPI who made this project possible.

## Executive Summary

Polarized cell growth is an essential process for the growth of many plant species. In the moss *Physcomitrella patens*, myosin XI has been implicated in polarized tip growth, which is the mechanism by which *P. patens* grows and expands. In 2010, Vidali et al. showed that a myosin XIa knockdown results in a distinctive phenotype in which polarized tip growth is inhibited, resulting in plants that are not branched. (Vidali et al. 2010). Myosin XI, a molecular motor that moves on actin tracts, has been hypothesized to be important for polarized growth by transporting secretory vesicles to the tip of expanding moss cells. These secretory vesicles are thought to contain cell wall and plasma membrane components that become part of the expanding cell tip. In *Arabidopsis thaliana*, it has been shown that the GTPase, RabA4, is also essential for polarized tip growth in pollen tubes and root hairs (Szumlanski and Nielsen 2009; Preuss et al. 2004). Moreover, in yeast, it has been shown that myo2p (the yeast protein that belongs to the myosin V family which is closely related to the plant myosin XI) interacts with several Rab proteins (Ypt31/32p and Sec4p) to mediate the transport of secretory vesicles (Lipatova et al., 2008; Santiago-Tirado et al. 2011; Jin et al., 2011). Therefore, in this study, it has been hypothesized that myosin XI transports secretory vesicles to the tip of expanding moss cells via an interaction with RabA4, the plant homolog of Ypt32p.

In this study, nine residues in the globular tail of myosin XI were identified as putative binding sites for an interaction with RabA4 via a comparison of a 3D model of the moss myosin XI with a yeast myosin globular tail crystal structure. To determine if each mutated myosin protein could rescue the myosin XI knockdown phenotype, the *P. patens* was simultaneously transformed with myosin XIa RNAi and each of the mutant myosin XIa constructs. Three mutations, L1306R, Y1397R and W1408R, complemented the myosin XI RNAi knockdown

phenotype, suggesting that they are not important residues for the binding of myosin XIa to RabA4. Conversely, the remaining six mutations did not complement the knockdown phenotype, suggesting they play some role in the binding of myosin XIa to RabA4. Three of these residues, F1379R, V1422R and V1418R, showed a phenotype that was identical to the RNAi knockdown phenotype, suggesting that they are very important for the binding of myosin XIa to RabA4, and the other three mutants, K1308E, Y1384R and H1394R only partially complemented the phenotype, suggesting that these residues may be important but not as essential.

These results do not definitively demonstrate that there is a direct interaction between the globular tail of myosin XIa and RabA4. Before this interaction can be confirmed, several other experiments need to be performed. To confirm that the mutated myosin constructs are being translated and protein is being produced, each mutant construct will be fused to 3mEGFP. Then, EGFP levels will be measured in moss cells transformed with the mutated 3mEGFP-myosin constructs and moss cells transformed with a 3mEGFP-myosin cDNA control. Secondly, pull down experiments will be performed to show that RabA4 directly interacts with wild type myosin XIa but does not interact with the mutated myosin constructs.

Overall, the results of this study will help to better understand polarized tip growth, and thus plant growth as a whole.

## Table of Contents

Abstract.....	ii
Acknowledgements.....	iii
Executive Summary .....	iv
Chapter 1: Introduction.....	1
Chapter 2: Background and Literature Review .....	3
2.1: The Actin Cytoskeleton.....	3
2.1.1: General characteristics of the actin cytoskeleton .....	3
2.1.2: Formins and Profilin.....	4
2.2: Myosin XI .....	4
2.2.1: General Characteristics of myosin XI .....	4
2.2.2: Function of myosin XI in polarized tip growth.....	6
2.2.3: PI4P .....	7
2.3: Rab proteins .....	8
2.3.1: General Characteristics of Rab proteins .....	8
2.3.2: Rab Proteins in Polarized Tip Growth.....	9
2.3.3: Rab Protein interaction with the tail of myosin XI.....	10
2.3.4: Regulation.....	11
2.4: Implications for this Study.....	11
Chapter 3: Materials and Methods.....	13
3.1: Generation of Mutations into the globular tail domain of myosin XIa.....	13
3.2: Transient transformation of <i>P. patens</i> with RNAi knockdown .....	15
3.3: Microscopy.....	16
3.4: Analysis of Pictures using Image J .....	17
3.5: Establishment of Baseline GFP levels .....	17
Chapter 4: Results.....	19
Chapter 5: Discussion and Suggestions for Future Study.....	29
References.....	34

## Chapter 1: Introduction

Polarized growth is essential for many processes in living organisms ranging from fungi to animals to plants. The fungi *S. cerevisiae*, otherwise known as budding yeast, accomplishes cell division in a polarized fashion. To divide, a budding daughter cell grows from and buds off from the mother cell (Johnston et al. 1991). In the animal model *Xenopus laevis*, eggs depend on polarized separation of yoke protein to establish the yolk gradient during embryogenesis (Danilchik and Gerhart 1987). Like in fungi and in animals, there are abundant examples of polarized growth in plants. In flowering plants such as *Arabidopsis thaliana*, pollen tube growth, and thus fertilization, is dependent upon polarized tip growth. Root hair growth also occurs in a polarized fashion in higher plants (Preuss et al. 2004). In polarized tip growth, expansion of the cell occurs only at the tip (Szumlanski and Nielsen 2009). This expansion is rapid and is accomplished by vesicular transport of membrane and cell wall components to the growing tip via exocytosis (Saito and Ueda 2009). Polarized tip growth is also essential for non-flowering plants, such as the moss *Physcomitrella patens*, which expands via this process (Menand et al. 2007).

*P. patens* is an ideal model to study polarized tip growth for many reasons. It grows quickly and is easy to manipulate. Like other mosses, it spends most of its life cycle in the protonemal (haploid) stage, so mutagenesis results directly in mutant phenotypes that are immediately visible. *P. patens* is able to be transformed both transiently and stably, allowing for the addition of plasmid DNA that has been manipulated in the lab (Goffinet & Shaw 2008). Moreover, because the genome of *P. patens* has recently been sequenced (Rensing et al. 2008), genetic manipulation is both possible and fairly straight forward. Additionally, unlike most

flowering plants, *P. patens* can undergo gene targeting via homologous recombination (Goffinet and Shaw 2008).

## Chapter 2: Background and Literature Review

### 2.1: The Actin Cytoskeleton

#### 2.1.1: General characteristics of the actin cytoskeleton

The actin cytoskeleton provides many functions to cells in *P. patens*, such as motility and more importantly, polarity. Myosin, a molecular motor, moves on actin filament tracts to transport cargo in a polarized fashion within the cell. Therefore, F-actin can be considered a key component of polarized growth within moss cells. However, in order to mediate polarized growth, actin needs to grow and shorten in order to fit the needs of the cell. Actin dynamics are based on different processes such as nucleation, elongation, treadmilling, fragmentation and bundle formation to dynamically grow and shrink within the cell. In nucleation, actin monomers assemble in dimers and then trimers (both of which are unstable). In elongation, these trimers extend rapidly to form a long polymer of F-actin (Blanchoin et al. 2010). In treadmilling, the length of a F-actin polymer stays virtually the same because the loss of actin monomers at one end of the polymer is equal to the rate of addition of new monomer at the other end of the polymer. Consequently, actin dynamics are dependent on many components including the concentration of free monomer available within the cell. Recently, it has been possible to study actin dynamics more thoroughly because of advances such as total internal reflection fluorescence microscopy and tagging with probes such as GFP and Lifeact (Blanchoin et al. 2010; Vidali et al. 2009a).

Plant model systems have many advantages over animal and microbial systems for studying the cytoskeleton for many reasons. These advantages include the fact that the fastest myosin motors are found plants (travelling at up to  $7.7 \pm 0.5 \mu\text{m/s}$ ) and that plants have novel actin-binding proteins (such as actin binding kinesins) (Blanchoin et al. 2010; Tominaga et al.

2003). Therefore, *Physcomitrella patens* is an ideal system to study polarized growth. Polarized growth is a complicated process and if it is to be understood, all components, including the role of actin, needs to be comprehensively studied.

### **2.1.2: Formins and Profilin**

Other known players in polarized tip growth in *P. patens* are formin proteins and profilin. Both of these proteins interact with actin to regulate its dynamics. Actin elongation is thought to be accelerated by proteins call formins (Blanchoin et al. 2010). In their 2009 study, Vidali et al. demonstrate that silencing of class 2 formins in *P. patens* results in spherical plants that lack polarized growth (Vidali et al. 2009b). Because formins mediate actin elongation, these results suggest that class 2 formins and rapid actin elongation are essential for polarized tip growth in *P. patens*. Profilin is a major actin binding protein that is found in moss. When the three isomers of profilin are knocked down using RNAi strategy, a complete loss of polarized tip growth is observed (Vidali et al. 2007).

## **2.2: Myosin XI**

### **2.2.1: General Characteristics of myosin XI**

Another protein implicated in the polarized tip growth of *P. patens* is myosin XI. Myosin XI is a molecular motor that moves along actin filaments. Although plant myosins can be split into three classes, land plants have two classes of myosins: class VIII and class XI (see figure 1). Myosin XI is most closely related to myosin V, which is found in animals and fungi (see figure 1) (Sparkes 2010).

In the moss *P. patens*, there are two isoforms of myosin XI: myosin XIa and myosin XIb. In vascular plants, the myosin XI class contains 13 isoforms that localize to various locations

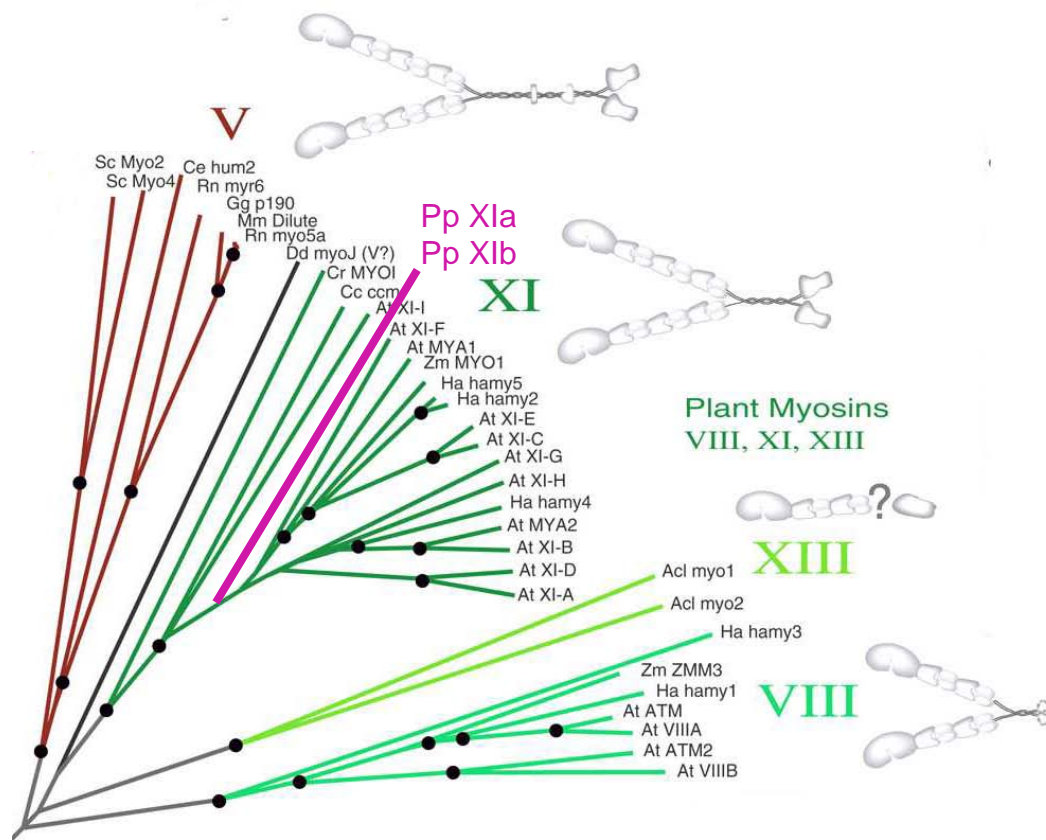


**Figure 1: Phylogenetic Tree of myosin proteins, highlighting plant myosins VIII, (XI and XIII) and the close relationship between myosin XI and myosin V. Taken from:**  
<http://jcs.biologists.org/content/suppl/2001/06/14/113.19.3353.DC1/jcs8504.pdf>

within the cell including motile puncta, the nuclear envelope, peroxisomes, Golgi bodies, F-actin, the ER and various locations throughout the cytosol (Sparkes 2010). As seen in figure 2, myosin XI, like myosin V, has four distinct domains: a head region, a neck region, a coil-coil region and a tail region and exists as a dimer. Myosin uses the head domain, or motor domain, to move along actin filaments via the hydrolysis of ATP. The coil-coil domain is essential for dimerization of myosin XI. The globular tail of myosin XI is associated with cargo (Sparkes 2010).

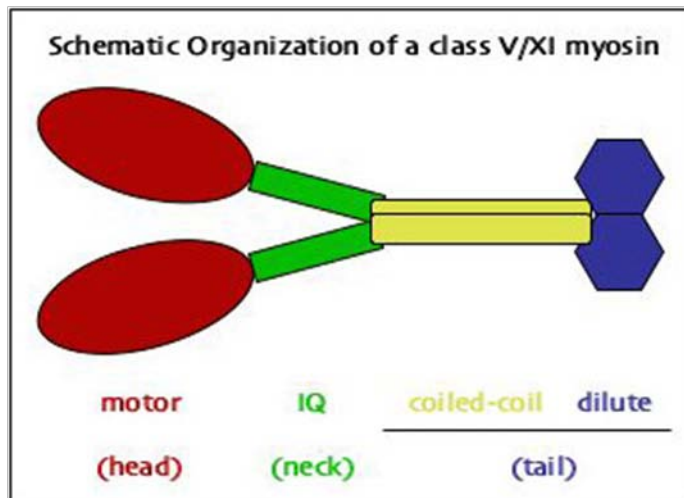


Figure 2: Basic domains of a class V/XI myosin motor. Taken from: <http://www.bio.utk.edu/cellbiol/res/myosin.htm>

### 2.2.2: Function of myosin XI in polarized tip growth

There are many lines of evidence suggesting that in some plant species, myosin XI may be essential for the movement of organelles (Avisar et al. 2008; Peremyslov et al. 2010; Peremyslov et al. 2008). Through the creation of a homology model, Li and Nebenführ conclude that the globular tail domain of the *A. thaliana* myosin XI resembles that of myosin V despite the low sequence similarity, suggesting that like myosin V, myosin XI could possibly be responsible for the movement of organelles. This resemblance may be due to the fact that 78% of the conserved residues are buried, suggesting that the residues important for folding were conserved. Li and Nebenführ also conclude that two subdomains within the myosin XI globular tail interact with one another both *in vitro* and *in vivo*, and that are each sufficient for organelle binding. Moreover, each subdomain targeted to different organelles, thus suggesting that they have independent cargo-binding sites. The authors suggest that this alternate binding may be due to myosin's ability to change the conformation of its globular tail, exposing different binding sites. Finally, the authors demonstrate that a sequence upstream of the globular tail, in the coil-coil

region, is crucial for proper folding of the globular tail (Li and Nebenführ, 2007). Because organelle movement is essential for the establishment of a polarized gradient of organelles in polarized tip growth, if myosin XI is important for organelle movement in *A. thaliana* then it could be also important for polarized tip growth (Peremyslov et al. 2008).

In addition, there are many lines of evidence that myosin XI is essential for polarized tip growth of *Physcomitrella patens*. Through RNAi silencing and complementation for loss of function, Vidali et al. demonstrated that the two myosin XI genes in *P. patens* are not only necessary for polarized tip growth, but are functionally redundant. They also show that myosin XI localizes in the tip of growing protonemal cells in a spot that is dynamic and has varying intensity, again suggesting that is important for polarized tip growth (Vidali et al. 2010). In this paper, the authors hypothesize that myosin XI either organizes the F-actin network or transports necessary material to and from the tip of the growing cell. This transport may possibly be done via secretory vesicles (Vidali et al., 2010). Also, in *Arabidopsis*, there seems to be a correlation between lack of polarized tip growth and deficiency in movement of organelles and secretory vesicles within the cell (Peremyslov 2008); therefore, it has been hypothesized that myosins are essential for tip growth because they transport secretory vesicles and organelles to the tip of the growing cell (Sparkes, 2010). In fact, Myo2p (that belongs to yeast myosin V family) has been shown to transport vesicles in a vectorial fashion (Johnson et al. 1991). Because myosin V and myosin XI are so closely related, myosin XI may perform a similar function in plants.

### 2.2.3: PI4P

Polarized tip growth obviously is a complex process that involves many factors that have not yet been discussed. For instance, in yeast, phosphatidylinositol 4-phosphate (PI4P) has been shown to be essential for the transport of secretory vesicles by Myo2p (Santiago-Tirado et al.

2011). PI4P is a lipid molecule that is often associated with membrane bound vesicles. Interestingly, the authors determined that PI4P was not binding directly to the tail but instead suggested that they were interacting via an adaptor protein. Furthermore, they showed that if PI4P is fused directly to Myo2p, the interaction of Myo2p with Ypt31/32p (Rab Proteins) and Sec4p is no longer needed (i.e. it is bypassed). In conclusion, the authors demonstrate that PI4P is critical for transport of secretory vesicles by Myo2p and that there are other contributing factors such as an adaptor protein, Sec4p and Rab Proteins. Phosphoinositides have also been shown to play a role in polarized tip growth in plants (Zhao et al. 2010).

## **2.3: Rab proteins**

### **2.3.1: General Characteristics of Rab proteins**

Rab proteins are also essential for polarized growth. These protein families play a critical role in vesicle/organelle transport and identification within the plant cell. Rab proteins are GTPases that act to target and/or tether cellular components to a target location within the cell. GTPases function by hydrolyzing GTP to GDP and can be regulated by other factors such as GTPase activating proteins (GAP) and guanine nucleotide exchange factor (GEF). After Rab proteins target cellular components to a target location, the SNARE proteins act to facilitate membrane fusion at the target membrane. Rab proteins are also thought to play a role in other processes such as membrane trafficking, gravitropism, autophagy, and tip growth (Satio and Ueda 2009). Rab proteins are thought to regulate tip growth in a spatio-temporal fashion by controlling what cargo is bound to myosin at any given time (Satio and Ueda 2009). Although Rab proteins have been implicated in tip growth, there is currently no evidence that SNARE proteins function in tip growth (Satio and Ueda 2009).

### 2.3.2: Rab Proteins in Polarized Tip Growth

There are many instances in which Rab proteins have been associated with polarized growth in plants. In tobacco, a pollen predominant Rab protein, NtRab2, has been implicated in pollen tube growth, which occurs via polarized tip growth (Cheung et al. 2002). NtRab2 was shown to function in a secretory pathway between the endoplasmic reticulum and the Golgi and was shown, via fusion with green fluorescent protein (GFP), to localize to the Golgi bodies. Interestingly, a dominant negative mutation of NtRab2, which inhibited the localization of the GFP fusion protein to the Golgi bodies, resulted in lack of transport between the endoplasmic reticulum and the Golgi bodies and the loss of pollen tube growth. Together, these results suggest that in tobacco, NtRab2 is essential for pollen tube growth, suggesting that Rab proteins may be a player in polarized tip growth.

In *A. thaliana* RabA4 has been shown to be essential for polarized tip growth in root hairs (Preuss et al. 2004; Thole et al. 2008) and pollen tubes (Szumlanski and Nielsen 2009). In root hairs, RabA4 has been shown to recruit effector molecules, such as the plant phosphatidylinositol 4-OH kinase, PI-4K $\beta$ 1 (Preuss et al. 2004). Moreover, when the gene for RabA4 in *Arabidopsis* was disrupted, pollen tube grew in a bulging, rather than linear, fashion. Therefore, this evidence suggests that the gene is not essential for general pollen tube growth but instead only growth in a polarized fashion. The mutant phenotype was able to be rescued by the addition of a functional RabA4d gene product. In addition, through fusions to EYFP, the authors were able to prove that RabA4d localizes at the tip of pollen tubes. Finally, the authors conclude that this protein is not involved in an endocytic process but instead is essential for the deposition of cell wall components to the tip of the growing cells. The authors make this conclusion because in the RabA4d mutant, cell expansion still takes place in a non polarized fashion and localization of

pectin is altered. Because the tip of the pollen tube is primarily formed of pectin, it is logical to assume that RabA4d may be responsible for transported pectin to the tip of a growing pollen tube. (Szumlanski and Nielsen 2009). These results, and the results from Cheung et al., suggest that Rab proteins are essential for polarized growth in plants.

### **2.3.3: Rab Protein interaction with the tail of myosin XI**

Rab proteins are thought to function in polarized tip growth in plants via a direct interaction with the myosin XI tail. This has been shown to be the case in yeast (Santiago-Tirado et al. 2011; Lipatova et al. 2008; Jin et al. 2011). Lipatova et al. (2008) conclude that the direct interaction between the yeast Myo2p globular tail (a yeast homolog of the animal myosin V) and the Rab molecule pair Ypt31/32p is required for polarized secretion. Furthermore, they show that Ypt31/32p must be bound to GTP for the interaction to successfully take place by performing two-hybrid assays with Ypt31/32p bound to GDP, GTP, and free of nucleotides. In addition, the authors identify the residues on Myo2p (L1411, Q1447 and Y1415) which are essential for this interaction. When these residues are mutated, the tail of myosin XI does not interact with Ypt31p or Ypt32p. Moreover, two residues (L1331 and K1444) are identified which, when mutated, do not interact only with Ypt32p but not Ypt31p. Finally, the authors conclude that this interaction is essential for the formation of trans-Golgi vesicles and for their motility (Lipatova et al. 2008). These results suggest that an interaction between the tail of myosin XI and Rab proteins may also be essential for polarized tip growth in the moss *P. patens*. In this project, it would be interesting to further explore the moss homologs of these residues to determine if they too are essential for the binding of RabA4d to the myosin XI tail.

### 2.3.4: Regulation

Regulation of biological processes is extremely important and regulation of the myosin tail could directly affect the putative interaction between myosin XI and RabA4. In yeast, the Myo2p protein has been shown to be phosphorylated, suggesting a possible regulation method (Legesse-Miller et al. 2006). Likewise, through alpha factor treatment, Legesse-Miller et al. also show that this phosphorylation is cell cycle dependent. Through mass spectrometry, the authors identify the phosphorylated residues and conclude that at any given time, 30% of the Myo2p tail is singly phosphorylated, 10% is doubly phosphorylated and 60% is unphosphorylated. Finally, the authors are able to demonstrate that PKA, a protein kinase, most likely plays a part in the phosphorylation of these residues (Legesse-Miller et al. 2006). Although the authors are unable to demonstrate any implications of these phosphorylation and dephosphorylation actions, understanding the regulation of Myo2p and other related myosin proteins is essential for understanding polarized tip growth as a whole.

### 2.4: Implications for this Study

As previously demonstrated, polarized tip growth is a complex process that is dependent on many factors. Several known players of polarized tip growth in the moss *Physcomitrella patens* include myosin XI (Vidali et al. 2010), F-actin and class II formins (Vidali et al. 2009b), and profilin (Vidali et al. 2007). In other plant organisms such as *A. thaliana* (Szumlanski and Nielsen 2009) and tobacco (Cheung et al. 2002), Rab proteins have also proved essential in polarized growth. Finally, in yeast, Rab proteins interact with the globular tail of myosin to mediate transport of secretory vesicles and organelles to the tip of cells expanding by tip growth (Lipatova et al. 2008). All of this taken together suggests that like in yeast, an interaction between the globular tail of myosin XI and a Rab protein may mediate polarized tip growth in

*Physcomitrella patens*. This study is designed to determine if polarized tip growth in *Physcomitrella patens* is mediated by the interaction between the globular tail of myosin XIa and the GTPase, RabA4. It is hypothesized that this interaction would allow myosin XIa to transport cargo, such as secretory vesicles and organelles to the tip of a growing moss cell via actin fibers.

## Chapter 3: Materials and Methods

### 3.1: Generation of Mutations into the globular tail domain of myosin XIa

Mutations were introduced to the *Physcomitrella patens* myosin XIa cDNA by PCR using mutagenic primers and a protocol adapted from the vendor (Finzymes). The primers used to generate each mutation can be seen in table one. The template used for PCR was a Gateway entry clone encoding the globular tail domain of myosin XIa. PCR bands were verified on a 0.8% (w/v) agarose gel. All electrophoresis gels were run at 220V for 19 minutes using a Bio-RAD 3000Xi power supply and a Liberty80 chamber from Biokeystone Co. The DNA was regained via gel purification using the NucleoSpin Extract II kit from Macherey-Nagel.

Plasmids containing the mutated myosin XIa tails were transformed into competent *E. coli* TOP 10 *shot* via a 30 second heat shock at 42°C and cells were grown overnight at 37°C on Petri dishes supplemented with 50 µg/ml kanamycin. Colonies containing the plasmid were selected by kanamycin resistance. The resulting plasmid DNA was amplified via a mini prep (from the NucleoSpin Plasmid kit from Macherey-Nagel) using an overnight 5 mL LB culture (cells were grown at 37°C for 16 hours). The DNA was screened via restriction enzyme digestion with AlfII and NotI and gel electrophoresis on a 0.8% (w/v) agarose gel. DNA was quantified by spectrophotometry. Absorbance values were read at 260nm and DNA was quantified assuming that at an optical density of one, the concentration of DNA was 50 ng/µl. Mutations were then verified using DNA sequencing at the Massachusetts General Hospital sequencing core. The primers used for sequencing can be found in table 1.

Table 1: All primers used in mutagenic PCR and sequencing.

Primer Name	Primer Sequence 5' to 3'	Primer Type	Used in:
<b>MyoXIAL1306RF</b>	AAGGGCAAGTCGCGGGAAGGTTTCAAGGTCACC	Forward Primer for L1306R	Mutagenic PCR
<b>MyoXIAK1308ER/L1306R R</b>	TGAGGTCCTTGGTGCCTGGATACAGAGCCCAAGC	Reverse Primer for L1306R/K1308E	Mutagenic PCR
<b>MyoXIAK1308EF</b>	AGGGCAAGTCTCGGGGAGGTTTCAAGGTCACCAA	Forward Primer for K1308E	Mutagenic PCR
<b>MyoXIAY1384RR</b>	TGAGCAACACTCACGTCTCAGCAGCAAAGTGT	Reverse Primer for Y1384R	Mutagenic PCR
<b>MyoXIAY1384RF</b>	TTAGCAACGGAGAGCGTGTGAAAGCTGGACTT	Forward Primer for Y1384R	Mutagenic PCR
<b>MyoXIAY1397RR</b>	TTCTGCAAGTCCAGCTTTCACATACTCTCCGTTGC	Reverse Primer for Y1397R	Mutagenic PCR
<b>MyoXIAY1397RF</b>	CTAGAGCACTGGATTCGTGAAGCTGGGGAGGAG	Forward Primer for Y1397R	Mutagenic PCR
<b>MyoXIAH1394RR</b>	TCCAGCTTTCACATACTCTCCGTTGCTAAATGA	Reverse Primer for H1394R	Mutagenic PCR
<b>MyoXIAH1394RF</b>	CTTGCAAGTCCAGCTTTCACATACTCTCCGTTGC	Forward Primer for H1394R	Mutagenic PCR
<b>MyoXIAV1418RF</b>	TATATCCGACAAGCACGTGGATTTTTGGTCATTCA -TC	Forward Primer for V1418R	Mutagenic PCR
<b>MyoXIAV1418RR</b>	CTTGAGCTCATCCCATGACGCTCCAGCATACTC	Reverse Primer for V1418R	Mutagenic PCR
<b>MyoXIAW1408RF</b>	TATGCTGGAGCGTCACGGGATGAGCTCAAGTAT	Forward Primer for W1408R	Mutagenic PCR
<b>MyoXIAW1408RR</b>	CTCCTCCCCAGCTTCATAAATCCAGTGCTCTAGTTC -TG	Reverse Primer for W1408R	Mutagenic PCR
<b>MyoXIAV1422RR</b>	TTGTCGGATATACTTGAGCTCATCCCATGACGCTC- C	Reverse Primer for V1422R	Mutagenic PCR
<b>MyoXIAV1422RF</b>	GCAGTTGGATTTTTGCGCATTATCAAAGCCA	Forward Primer for V1422R	Mutagenic PCR
<b>MyoXIAF1379RR</b>	TCTCAGCAGCAAAGTGTGAACAGCTGAACATT	Reverse Primer for F1379R	Mutagenic PCR
<b>MyoXIAF1379RF</b>	CGTGAGTGTGCTCACGTAGCAACGGAGAGTAT	Forward Primer for F1379R	Mutagenic PCR
<b>UMASS397</b>	TGGAGGTGCTCCTCAAAGACG	Used for all mutations	sequencing
<b>WPI34</b>	GGGGACAACCTTTGTATAC- AAAGTTGTAGAATCTGGTTGTGGCATTAG	Reverse Primer for all mutations	PCR
<b>WPI36</b>	GGGGACAAGTTTGTACAAAAAGC- AGGCTTAATGGCGACAGCGGAATGTA	Forward Primer for all mutations	PCR

LR reactions were performed to combine the entry clones containing the mutated globular tail domains in the second position with an entry clone containing the head, neck and coil-coil domains of myosin XIa in the first position of the Gateway system. The destination vector for this reaction was pTHUbi-gate R1R2. The resulting expression vectors were transformed into competent *E. coli TOP 10 shot* and grown overnight, for 16 hours, at 37°C. Colonies containing the desired DNA were selected for carbenicillin resistance on Petri dishes supplemented with 100 µg/ml carbenicillin. DNA was amplified via a mini prep from 2 ml LB starters, grown overnight for 16 hours at 37°C, and was quantified using spectrophotometry. The correct DNA constructs were verified via restriction enzyme digestion with PvuII and gel electrophoresis on a 0.8% (w/v) agarose gel.

To obtain larger amounts of plasmid DNA, a 2 mL LB starter was inoculated with *E. coli* transformed with the desired DNA and grown overnight for 16 hours at 37°C. A second 2 mL LB starter was then inoculated from 100 µl of the first starter and grown at 37°C for about 8-10 hours. Finally, a 250 mL terrific broth culture was inoculated with the entire 2 mL starter and cells were grown overnight for 16 hours at 37°C. This terrific broth culture was then used to perform a maxi prep to obtain DNA at a concentration  $\sim > 1 \mu\text{g}/\mu\text{l}$ . Maxi preps were performed using the Nucleo Bond Xtra Maxi kit from Macherey-Nagel.

### **3.2: Transient transformation of *P. patens* with RNAi knockdown**

To transform *P. patens* with plasmids containing the DNA of interest, two plates of moss (grown for 7 days) were first protoplasted for one hour in a solution of 3 mL of 2% (w/v) Driselase and 9 ml of 8% (w/v) mannitol (Liu and Vidali 2011). The moss strain used was MBNLS4 which has a GFP-GUS fusion that localizes to the nucleus via a nuclear localization sequence (Vidali et al. 2007). After one hour, the protoplasts were filtered and any residual enzyme was removed with

a series of washes with 8% (w/v) mannitol. The number of protoplasts was then quantified with a hemocytometer, and the cells were then diluted with MMg buffer (0.4 M mannitol, 15 mM MgCl<sub>2</sub>, 4 mM MES (pH 5.7)) to a final concentration of 1.6 X 10<sup>6</sup> protoplasts/mL. After 20 minutes of incubation at room temperature, 30 µg of each construct was added to 300µl of protoplasts. After 30 minutes of incubation at room temperature with the DNA and 350µl of PEG6000/Ca<sup>2+</sup> (60% (w/v) PEG4000, 0.002 M mannitol, 0.01M CaCl<sub>2</sub>), the cells were diluted with 1.5ml of W5 buffer (154 mM NaCl, 125 mM CaCl<sub>2</sub>, 5 mM KCl, 2 mM MES (pH 5.7)) and then were centrifuged in a swing out rotor at 700rpm/250g for 5 minutes to remove the PEG. After being resuspended in 1 mL of PpNH<sub>4</sub> (1.03 mM MgSO<sub>4</sub>, 1.86 mM KH<sub>2</sub>PO<sub>4</sub>, 3.3 mM Ca(NO<sub>3</sub>)<sub>2</sub>, 45 mM FeSO<sub>4</sub>, 9.93 mM H<sub>3</sub>BO<sub>3</sub>, 220 nM CuSO<sub>4</sub>, 1.966 mM MnCl<sub>2</sub>, 231 nM CoCl<sub>2</sub>, 191 nM ZnSO<sub>4</sub>, 169 nM KI, 103nM Na<sub>2</sub>MoO<sub>4</sub>, and 2.72 mM diammonium tartrate )/8% (w/v) mannitol/10mM CaCl<sub>2</sub> (PPNH<sub>4</sub> with 8.5% (w/v) mannitol without agar, CaCl<sub>2</sub> added to 10µM before use), the protoplasts were then plated on PRMB medium (PPNH<sub>4</sub> with 6% (w/v) mannitol, 0.8% (w/v) agar, 10 mM CaCl<sub>2</sub>) plates for four days. On the fourth day, the moss was transferred to PpNH<sub>4</sub> + Hygromycin (15mg/L) plates (Liu and Vidali 2011).

### 3.3: Microscopy

Seven days after the transformation (three days after transfer to antibiotic selection), plants were observed under the microscope and photographed for further analysis. The microscope used was a Zeiss SteREO Discovery.V12, the camera used was AxioCamMR3 and the imaging software used was AxioVision. Plants were observed using a 10X objective on the microscope and photographed using 63X magnification. The filter used on the microscope was EGFP480 (Excitation 480/40, Dichroic 405 LP, Emission 510 LP).

### 3.4: Analysis of Pictures using Image J

Image J was used to analyze photographs taken under the microscope. First, the macro “Zeiss\_RGB\_Red\_green\_merger.txt” was used to merge all the channels from the photography software. Then, all the photographs of one sample were combined in a stack. The resulting file was saved as a .tif and then, the macro “Shaving\_Macro\_V2.0\_RGB.txt” was used to select the plant of interest. Once this was accomplished for all pictures in the file, the resulting file was saved without the .tif extension. This new file was then dumped into Image J and the macro “Morphological\_Macro\_V2.1\_Red.txt” was then used to analyze the photographs and put the resulting data in a Microsoft Access file. This macro determined the area and solidity of each plant. Solidity is a measure, from 0 to 1, of polarized growth based on the convex hull and area of a shape. A plant with a solidity of 0 is highly branched where as a plant with a solidity of 1 would not be branched.

### 3.5: Establishment of Baseline GFP levels

To determine if protein expression levels could be verified via protein fusion with a fluorescent protein, myosin XIa cDNA fused to 3mEGFP was transformed into *P. patens* using the procedure described above. The fluorescence intensity in these transformants was compared to that of plants transformed with only the cDNA construct. To accomplish this, photos were taken of one week old transformants that lacked nuclear GFP, indicating successful RNAi knockdown and thus a successful transformation. Photos were taken using both the EGFP480 filter (to capture both the chlorophyll and GFP fluorescence) and the GFP470 filter (to capture only GFP fluorescence). ImageJ was then used to first threshold the image of the plant using the chlorophyll signal and then calculate the average GFP expression/pixel. This value was

compared between the two groups to determine if this method could be used to determine if a protein was expressed.

## Chapter 4: Results

In order to study the putative interaction between the globular tail of myosin XI and

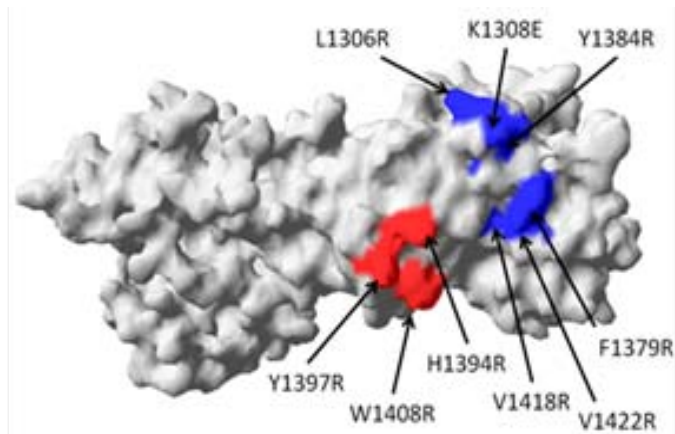


Figure 3: 3D Model of the globular tail of myosin XIa showing the putative interaction sites for the globular tail of the *P. patens* Myosin XIa globular tail and RabA4. Arrows indicate mutations made to interrupt this binding.

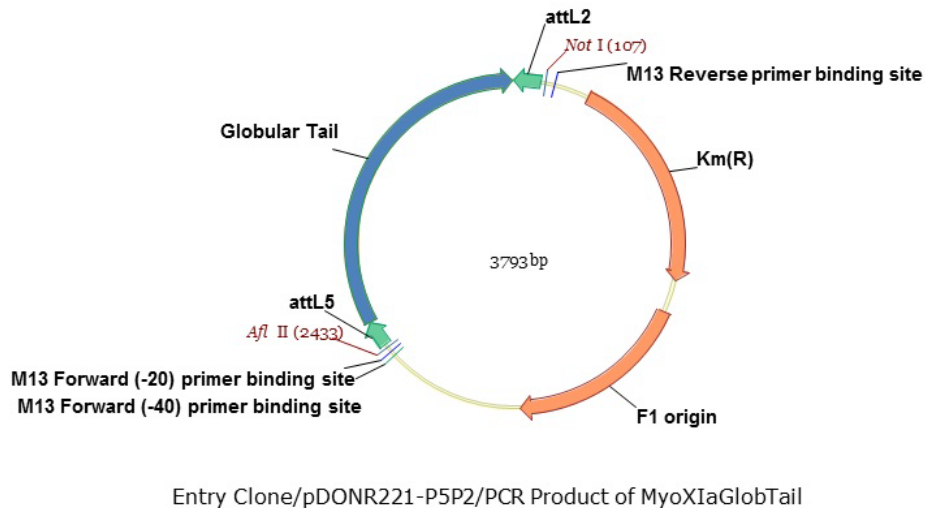
RabA4 in the moss *P. patens*, a mutagenic approach was chosen in order to attempt to disrupt this putative binding. To determine which amino acids to mutate to disrupt potential binding



Figure 4: PCR products analyzed via gel electrophoresis on a 0.8% (w/v) agarose gel.

between the globular tail of myosin XIa and RabA4 a 3D model of the *P. patens* myosin XI globular tail was compared to crystal structure of the yeast myosin V (a homolog of the plant myosin XI). It has previously been determined what residues are important for the binding of the myosin globular tail to Rab proteins to mediate secretory vesicle transport in yeast (Pashkova et al. 2006; Lipatova et al 2008; Jin et al 2011). As seen in figure 3, examination of this

comparison led to the proposal of nine potential amino acids that may be important for the binding of myosin XI to RabA4 in *P. patens*. In figure 3, both the red and blue coloration represent putative binding sites on the myosin globular tail for RabA4.



**Figure 5: Restriction Enzyme cut sites for all entry clones. All entry clones were screened with AflIII and NotI.**

To create these mutations in the globular tail of myosin XIa, mutagenic primers were designed for PCR (see table 1). To introduce the mutations into myosin XIa, mutagenic PCR was performed using an entry clone containing the globular tail of myosin XIa as a template and the products were run on a 0.8% (w/v) agarose gel. As seen in figure 4, all nine mutagenic products showed the expected band of ~3800 bps, similarly to the template.

The PCR products were gel purified and re-ligated to create circular plasmids. These plasmids were then transformed into *E. coli* and amplified via a mini prep. The integrity of this product was then verified by restriction enzyme digestion with NotI and AflIII and gel electrophoresis. A representative diagram of restriction enzyme digestion for all entry clones can be seen in figure 5 and the resulting gel for the entry clones can be seen in figure 6. As seen in figure 6, both constructs containing the L1306R and K1308E mutations produced the expected

bands (1467 bp and 2346 bp) for all tested clones. Expected bands were also produced for the other seven tail mutation constructs (data not shown).

Finally, to verify that the mutations were successfully introduced into the globular tail of myosin XIa, entry clones were sent for sequencing. Sequencing results representative of all of the mutations can be seen in figure 7. Figure 7 shows part of the sequence for the entry clones encoding the wild type globular tail of myosin XIa and the globular tail containing the L1306R mutation. As seen in the sequence, the mutagenesis was successful, changing a leucine to an

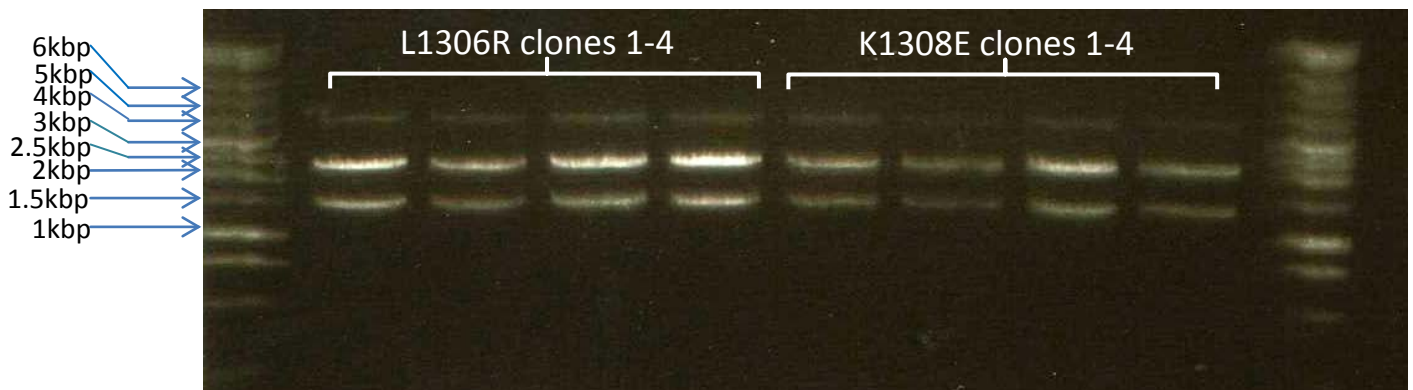


Figure 6: Representative Gel from digested entry clones containing the mutated globular tails. Lane 1=ladder, Lanes 2-5= pL1-Globtail-L1306R-R5 clones 1-4. Lanes 6-9= pL1-Globtail-K1308E-R5 clones 1-4. Lane 10=ladder.

arginine. Mutagenesis was equally successful for the other eight mutations (data not shown).

After the mutations were verified, an LR reaction was performed to combine the mutated globular tails with the head, neck and coil-coil of myosin XIa. This product was then transformed into *E. coli* and amplified via a mini prep. The DNA was analyzed via restriction

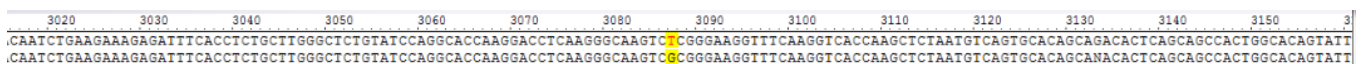
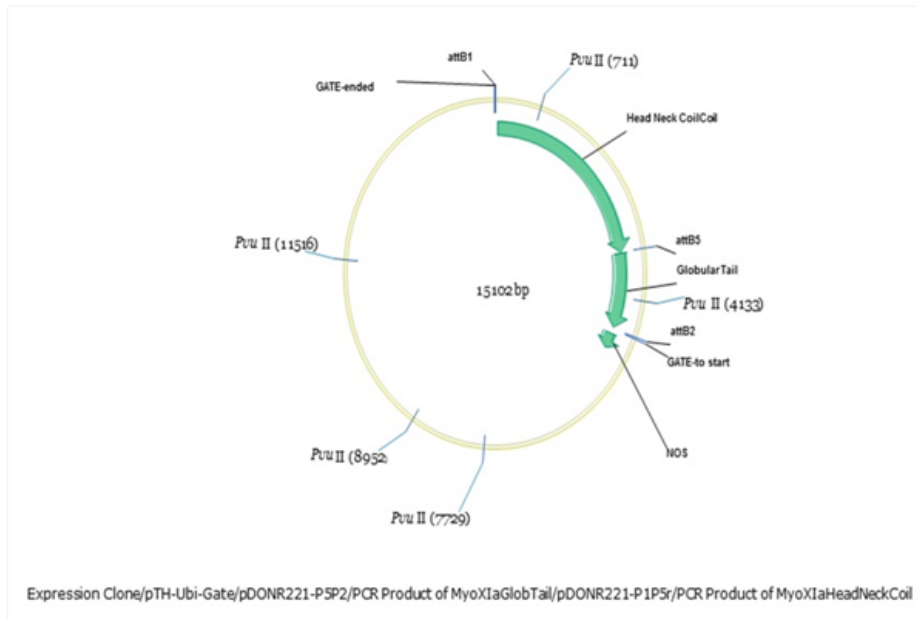


Figure 7: A portion of the alignment comparing the sequencing of pL1-MyoGlobtail-R5 (top) and pL1-MyoGlobtail-L1306R-R5 (bottom). The change of the codon CTC (Leucine) to CGC (Arginine) indicates a successful mutagenesis.

enzyme digestion with PvuII and gel electrophoresis. A representative diagram of the restriction enzyme digestion for all expression clones can be seen in figure 8 and the resulting gel for the expression clones can be seen in figure 9. As seen in figure 9, all expression clones containing the L1306R mutation produced the expected bands (1223 bp, 2562 bp, 3422 bp, 3596 bp and 4297 bp) when digested with PuvII. Digestion with PuvII of the other eight mutagenic expression vectors also produced the expected bands (data not shown).



**Figure 8: Restriction Enzyme Cut sites for all Expression Vectors. All expression vectors were screened with PuvII**

After amplifying all expression clones via maxi preps, the resulting DNA was co-transformed into the moss *P. patens* with a myosin XI RNAi construct that produces a tip growth phenotype and each mutant protein was investigated for complementation. In addition, each transformation was performed in parallel with a control RNAi construct to verify that the interference process occurs, and a myosin XI cDNA control that is able to complement the myosin XIa RNAi phenotype. To analyze the phenotype of each cell line, plants were imaged under a fluorescence stereomicroscope one week after transformation and the photos were

analyzed using Image J. Results from the transformations can be seen in figure 10. As seen in figure 10, when *P. patens* is transformed with myosin XI RNAi, polarized growth is highly affected and the transformed plants have less branched cells and show a high solidity phenotype. Moreover, as seen in figure 10, the myosin RNAi knockdown phenotype can be rescued with myosin XI cDNA. *P. patens* was then transformed with each of the nine mutant myosin XI constructs to see if they could rescue the myosin XI RNAi phenotype. If a mutant myosin XI construct failed to rescue the myosin RNAi knockdown phenotype, it is possible that the mutated residue could be essential for the putative interaction between myosin XI and RabA4.

When determining the effect of these mutations, two different parameters were investigated: area and solidity. Interestingly, eight of the nine mutations had an effect on the average area of the plant. Figure 11 shows the average area of each population tested. As seen in figure 11, only plants transformed with L1306R had an area that was not statically different that plants transformed with the myosin XI cDNA control. Similarly, as seen in table 2, when a Tukey one-way ANOVA was performed between all samples, all of the mutations were significantly different than the cDNA control except L1306R with respect to the natural log of the normalized area when  $p=0.001$ . In fact, many mutations had statistically significant values at even lower  $p$  values.

As seen in figures 10 and 12, six of the nine mutations (V1418R, V1422R, F1379R,

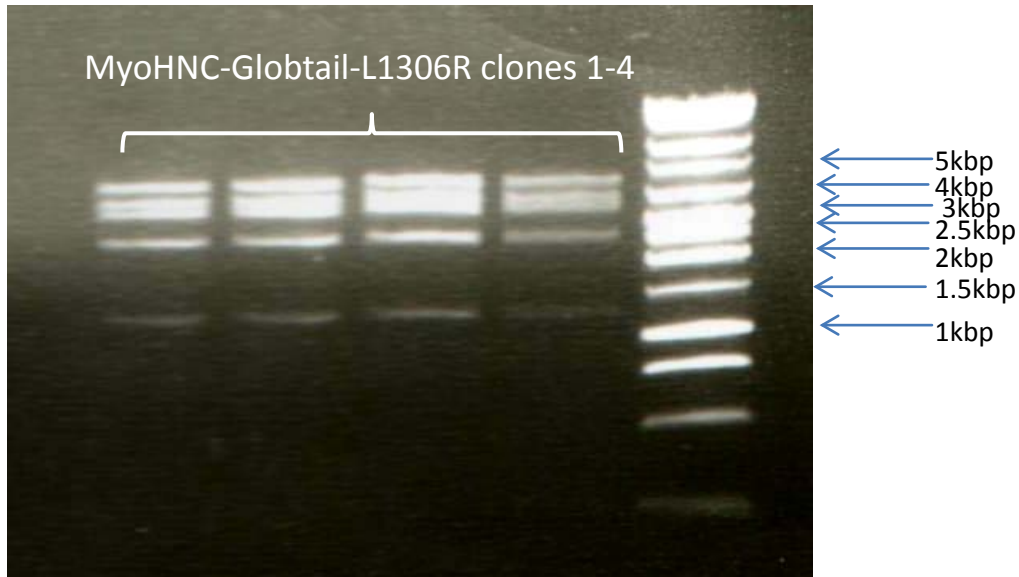


Figure 9: Representative gel for the analysis of expression vectors via digestion with PuvII. Lane 1= Ladder. Lanes 2-5= pB1-MyoHNC-B5-Globtail-L1306R-B2 clones 1-4.

H1394R, K1308E, Y1397R) failed to fully complement the solidity phenotype. Three of these mutations, V1418R, V1422R and F1379R, had the most extreme phenotype, similar to that of myosin XI RNAi. The K1308E, H1394R and Y1397R mutations showed intermediate tip growth phenotypes, suggesting that they were able to partially rescue the tip growth phenotype. As seen in figures 10 and 12, the remaining three mutations (L1306R, W1408R and Y1384R) were not statically different from the cDNA control, suggesting that, when their effect on solidity was evaluated, they successfully rescued the myosin RNAi knockdown phenotype. Table 3 shows the statistics for the solidity for each population that was tested. A one-way ANOVA (Tukey ANOVA) was performed. As seen in table 3, all mutations except L1306R, W1408R and Y1397R were statistically significant when compared with the cDNA control at  $p < 0.0001$  and many were statistically significant at much lower values.

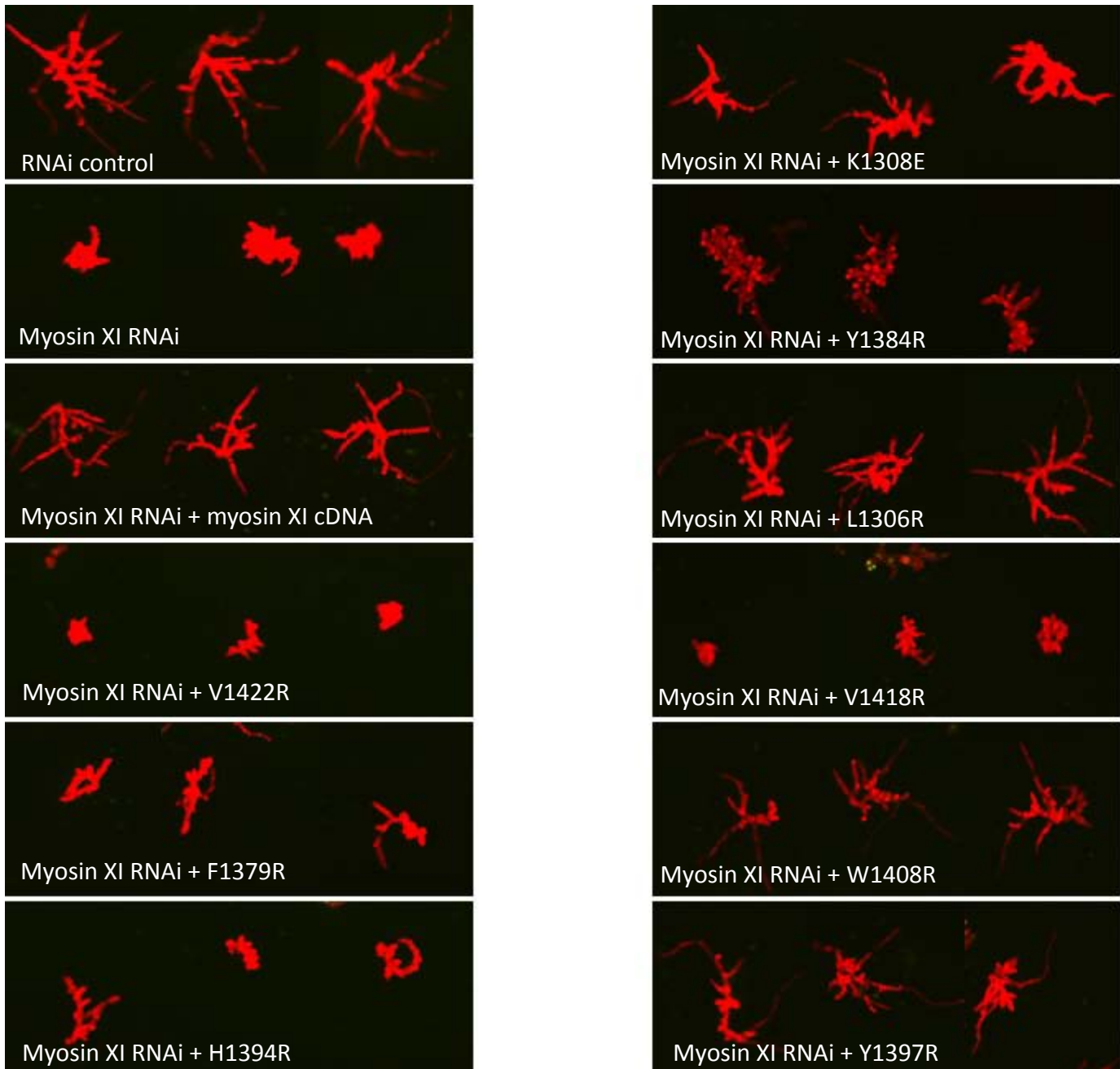


Figure 10: Three representative photos of *P. patens* transformed with each control and mutagenic myosin XIa.

Samples Compared	adjusted P value	Significant @ 0.05
L1306R vs. cDNA Control	0.99707	no
Y1384R vs. cDNA Control	<0.001	yes
H1394R vs. cDNA Control	<0.0001	yes
K1308E vs. cDNA Control	<0.0001	yes
W1408R vs. cDNA Control	<0.0001	yes
F1379R vs. cDNA Control	<0.0001	yes
Y1397R vs. cDNA Control	<0.0001	yes
V1422R vs. cDNA Control	<0.0001	yes
V1418R vs. cDNA Control	<0.0001	yes

Table 2: Tukey One-way ANOVA performed on the area data for all samples tested. Shown here is the adjusted p-value for each mutation when compared with the cDNA control.

Samples compared	adjusted P value	Significant @ 0.05
L1306R vs. cDNA Control	1	no
Y1384R vs. cDNA Control	<0.0001	yes
H1394R vs. cDNA Control	<0.0001	yes
K1308E vs. cDNA Control	<0.0001	yes
W1408R vs. cDNA Control	0.21021	no
F1379R vs. cDNA Control	<0.0001	yes
Y1397R vs. cDNA Control	0.15303	no
V1422R vs. cDNA Control	<0.0001	yes
V1418R vs. cDNA Control	<0.0001	yes

Table 3: Tukey One-way ANOVA performed on the natural log of the normalized solidity data for all samples tested. Shown are the adjusted p values for all mutations when tested against the cDNA control.

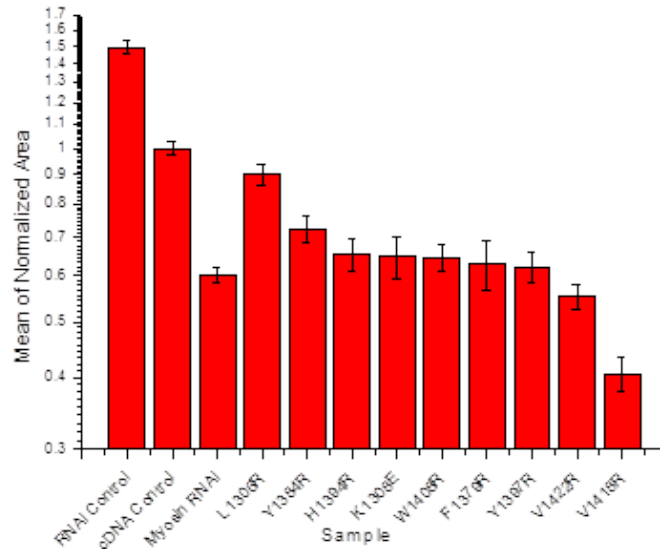


Figure 11: Average Normalized Area for each population tested. Whiskers represent the Standard Error.

In the future, to verify that the differences seen in complementation in the transformation experiments were due to the mutations and not due to lack of protein expression, the mutagenic constructs that did not fully rescue the myosin RNAi phenotype will be fused to 3mEGFP. To verify that differences in fluorescence levels between 3mGFP fused constructs and constructs not

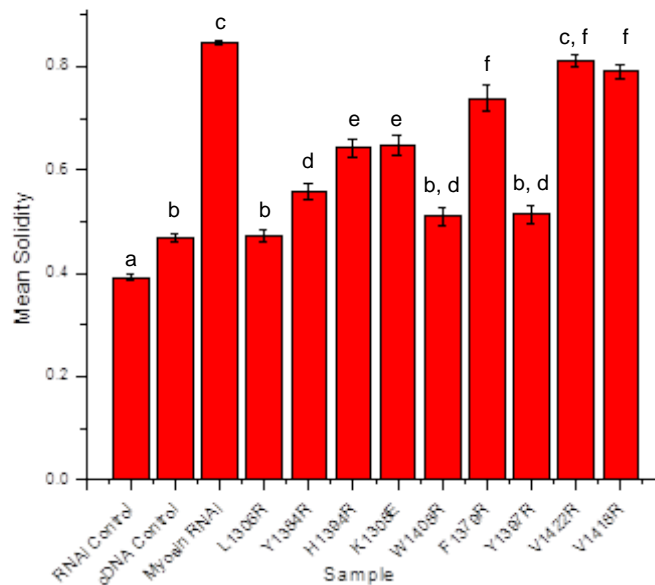


Figure 12: Average Solidity of each population tested. Whiskers represent the standard error of the mean. Statistics (lowercase letters) were done using a two way ANOVA test and post hoc Tukey test.

fused to GFP can be accurately measured, photos were taken of plants transformed with myosin XIa cDNA fused to 3mEGFP and plants transformed with myosin XIa cDNA alone. Fluorescence levels were measured using ImageJ and it was determined that there was a statistically significant difference between the two populations (t-test,  $p < 0.0002$ ). Figure 13 shows the differences in fluorescence level between the two populations. Because the difference between the two populations was statistically significant, it should be possible to determine if non-complementing mutants are expressed by fusing each construct to 3mEGFP and measuring the mean fluorescence levels of each transformant.

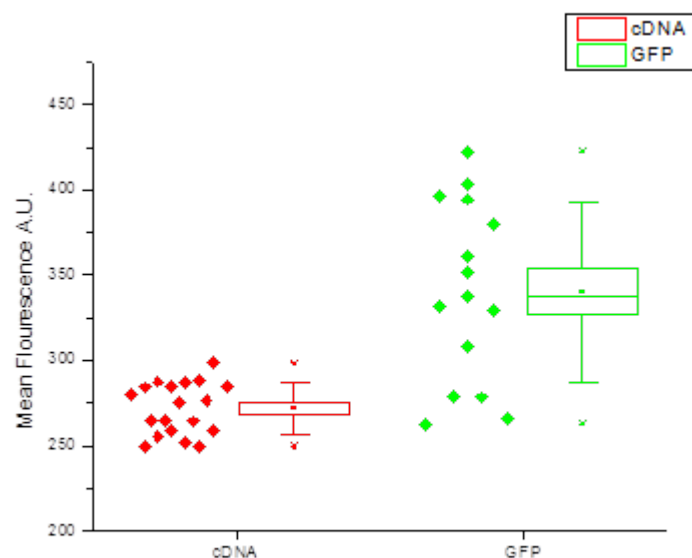


Figure 13: Graph depicting the mean fluorescence of plants transformed with myosin XIa cDNA and plants transformed with mEGFP fused to myosin XIa cDNA. Results were statistically significant at  $p < 0.0002$ , t-test.

## Chapter 5: Discussion and Suggestions for Future Study

Polarized tip growth is essential to the moss *Physcomitrella patens* for its growth and expansion. It has been hypothesized that polarized tip growth in *P. patens* occurs by transport, to the tip of expanding cells, of secretory vesicles containing cell wall and plasma membrane materials by myosin motors on F-actin tracts. Moreover, the myosin XI transport of secretory vesicles has been hypothesized to occur via an interaction with RabA4.

The results of this study, specifically those seen in figures 10-12, suggest that there is an interaction between the globular tail of myosin XIa and RabA4 in *Physcomitrella patens*. The residues that were mutated in this study were chosen because they corresponded to amino acids on the globular tail of myosin XI that, in yeast, are essential for the binding of myosin XI to secretory vesicles. Therefore, because mutations in these specific residues produced a phenotype very similar to the phenotype of a myosin XIa knockdown, it seems that, like in yeast, these residues are important for binding to RabA4. However, there are many caveats that need to be considered before this inference can be conclusively reached.

Six of the nine mutations tested were able to rescue the RNAi knockdown of myosin XI with varying degrees of success, but only three mutations (L1306R, W1408R, and Y1397R) were not statistically different to the cDNA control in respect to solidity. In this case, the results suggest that the six mutations that were statistically different than the cDNA control represent essential residues for the putative binding of myosin XI to RabA4 whereas the three complementing mutations represent nonessential residues. However, as seen in figures 10 and 12, of the six mutations that failed to complement, three did show some partial rescue (i.e. K1308E, Y1384R and H1394R). In fact, of the six non-complementing mutations, only V1422R was not statistically different than the myosin RNAi knockdown. Therefore, it seems as if some

residues in the binding region may be more crucial than others. To further explore this, double mutations could be made with the residues that partially complement to verify if the double mutations have a more severe phenotype.

Moreover, it should be noted that after the complementation experiments were completed, additional sequencing revealed that the H1394R construct had an additional mutation elsewhere in the sequence. Therefore, before this histidine can be accepted as an important residue for the myosin XI/ RabA4 interaction, a new construct needs to be made and the effect of the mutation in plant growth re-evaluated.

As seen in figure 3, five of the six non-complementing mutations (V1422R, V1418R, F1379R, K1308R and Y1384R) are located in the same region of the myosin XI globular tail. This seems to suggest that this region (highlighted in blue in figure 3) may be essential for the binding of myosin XI to RabA4. To further investigate this, it should be determined if these residues and this region of the myosin XI globular tail are conserved among other plant species. Additionally, the 3D model seen in figure 3 could also be used to determine additional residues that may be important for the binding of myosin XI to RabA4. If the region highlighted in blue is essential for this binding, then it is likely that other residues in this region may be important. These residues should be tested by complementation to determine their importance.

The mutations with the highest solidity values (V1418R, V1422R, F1379R) had a very pronounced phenotype that was very similar to the myosin XI knockdown phenotype and, therefore, logically seem to be the residues most important for the putative binding of the globular tail of myosin XI to RabA4. However, there are many other factors that should first be considered. It must be noted that valine is a nonpolar, hydrophobic amino acid, and thus is possible to be found at the core of the myosin XI globular tail. Therefore, mutating valine to

arginine, which is a more polar amino acid, may result in disruption of the amino acid structure of the tail domain of myosin XIa and not disruption of the putative binding site for RabA4. There are several techniques that could be performed to explore the conformation of the mutated myosin XI proteins with the valine to arginine mutations. One such technique could be running the wild type and mutated proteins on a urea-gradient denaturing-gel via electrophoresis. Because electrophoresis on this type of acrylamide gels separate proteins based on shape, if the two proteins are run side by side, a difference in stability should be easily discernible as a change in migration. To complement this method or if additional resolution was required, other more complicated techniques, such as circular dichromism, could be tried. This technique, which helps to determine secondary structures, would help to distinguish between a well folded protein and a misfolded protein.

Another alternative explanation for the mutations that fail to complement would be that these residues have another function (other than binding to RabA4) that when lost, causes a loss of polarized tip growth. To rule out this possibility, an immuno-precipitation experiment has been designed and will be performed after the completion of this study. In this experiment, the mutated globular tails of myosin XI will be fused to 3mEGFP and RabA4 will be fused to 3mCherry. The globular tail-3mEGFP constructs will be immobilized on a column containing superparamagnetic beads coated with an antibody to GFP by running moss extract (from a line that expresses 3mEGFP-Myosin-Tail and 3mCherry-RabA4) over the column. Then, the products will be eluted with an SDS-loading buffer and the resulting product will be run on an SDS-PAGE gel. Finally, a Western blot will be performed and probed with an antibody anti-RFP, which successfully detects the 3mCherry and anti-GFP to ensure that the 3mEGFP was properly immobilized. If the sample has a positive result for the antibody anti-RFP, then it can

be assumed that in that sample, there was an interaction between the globular tail of myosin XI and RabA4 and that the mutated residues are not important for the interaction. Similarly, if there is no signal on the western blot or if the signal is less than the control, it can be assumed that the mutated residues are important for the binding of the *P. patens* myosin XI globular tail to RabA4. However, because this method does not prove a direct or indirect interaction between the two proteins, both proteins will also be purified with GST and 6xHistidine tags to test for direct interactions via a pull-down experiment.

Finally, it is possible that the mutated myosin constructs fail to complement the RNAi myosin XI knockdown phenotype because no mutant protein is being produced. To test for this, each mutation that failed to complement will be fused to 3mEGFP and moss will be transformed with these constructs. Next, GFP fluorescence levels within the cell will be measured and compared to GFP fluorescence background levels from moss cells transformed with a cDNA control. As seen in figure 13, it has been determined that it is possible to discern a statistically significant difference in GFP fluorescence levels between moss transformed with a myosin XI cDNA control and moss transformed with myosin XI cDNA wild type fused to 3mEGFP. Moreover, this difference is statistically significant even at low n values (here  $n < 20$ ). Therefore, this method should be a successful, quantitative way to determine if mutant protein is being produced within the transformed cells.

Interestingly, some of the mutations that complemented the solidity phenotype did not have normal area values. As seen in figure 11 and table 2, only the L1308R mutation was able to successfully complement the area. The other 8 mutations had area values that were significantly different than the cDNA control. This makes sense for the six mutations (V1422R, V1418R, F1379R, H1394R, K1308R and Y1384R) that did not complement the solidity phenotype

because increased solidity logically suggests reduced area. However, for the remaining two mutations that complemented the solidity phenotype but did not complement the area, it becomes more interesting. Because these mutations show normal polarized growth but reduced growth overall, it seems as if polarized tip growth is not blocked but slowed down. In other words, mutations in these two residues may not inhibit polarized tip growth, but may instead, slow the whole process. Therefore, these residues need to be studied more closely as they may play some role in tip growth as a whole.

Overall, the results from this study seem to suggest an interaction between the globular tail of myosin XI and RabA4 in *Physcomitrella patens*. Because mutations in the putative binding site for RabA4 on the myosin XI tail shows a similar phenotype to a RNAi myosin XI knockdown mutant, it can be assumed that these residues are important to the myosin XI protein and for the binding of RabA4. However, before an interaction with RabA4 can be confirmed, there are still many other possible explanations for these results that need to be ruled out. On the other hand, if this interaction can be confirmed, we will be one step closer to understanding polarized tip growth as a whole.

## References

- Avisar, D., Abu-Abied, M., Belausov, E., Sadot, E., Hawes, C., Sparkes, I. (2009). A Comparative Study of the Involvement of the 17 Arabidopsis Myosin Family Members on the Motility of Golgi and Other Organelles. *Plant Physiology*, 150: 700-709.
- Avisar, D., Prokhnevsky, A., Makarova, K., Koonin, E., Dolja, V. (2008). Myosin XI-K Is Required for Rapid Trafficking of Golgi Stacks, Peroxisomes, and Mitochondria in Leaf Cells of *Nicotiana benthamiana*. *Plant Physiology*. 146 (3): 1098-1108.
- Blanchoin, L., Boujemaa-Paterski, R., Henty, J., Khurana, P., and Staiger, C. (2010). Actin dynamics in plant cells: a team effort from multiple proteins orchestrates this very fast-paced game. *Current Opinion in Plant Biology*, 13: 714-723.
- Cheung, A., Chen, C., Glaven, R., Graaf, B., Vidali, L., Hepler, P., Wu, H. (2002). Rab2 GTPase Regulates Vesicle Trafficking between the Endoplasmic Reticulum and the Golgi Bodies and Is Important to Pollen Tube Growth. *The Plant Cell*. 14: 945-962.
- Danilchik, M., and Gerhart, J. (1987). Differentiation of the animal-vegetal axis in *Xenopus laevis* oocytes\* 1::I. Polarized intracellular translocation of platelets establishes the yolk gradient. *Developmental Biology*. 122(1): 101-112.
- Goffinet, B., and Shaw, A.J. (ed). *Bryophyte Biology: Second Edition* Cambridge University Press, Cambridge. 2008.
- Jian-Feng, L. and Nebenführ, A. (2007). Organelle Targeting of Myosin XI is Mediated by Two Globular Tail Subdomains and Separate Cargo Binding Sites. *The Journal of Biological Chemistry*, 282(28): 20593-20602.
- Jian-Feng, L. and Nebenführ, A. (2008). The Tail that Wags the Dog: The Globular Tail Domain Defines the Function of Myosin V/XI. *Traffic*, 9: 290-298.

- Jin, Y., Sultana, A., Gandhi, P., Franklin, E., Hamamoto, S., Khan, A., Munson, M., Schekman, R., Weisman, L. (2011). Myosin V Transports Secretory Vesicles via a Rab GTPase Cascade and Interaction with the Exocyst Complex. *Developmental Cell*. 21(6): 1156-1170.
- Johnson, G., Prendergast, J., and Singer R. (1991). The *Saccharomyces cerevisiae* MYO2 Gene Encodes an Essential Myosin for Vectorial Transport of Vesicles. *The Journal of Cell Biology*, 113(3): 539-551.
- Legesse-Miller, A., Zhang, S., Santiago-Tirado, F., Van Pelt, C., and Bretscher, A. (2006). Regulated Phosphorylation of Budding Yeast's Essential Myosin V Heavy Chain, Myo2p. *Molecular Biology of the Cell*. 17: 1812-1821.
- Lipatova, Z., Tokarev, A., Jin, Y., Mulholland, J., Weisman, L., Segev, N. (2008). Direct Interaction between a Myosin V Motor and the Rab GTPases Ypt31/32 Is Required for Polarized Secretion. *Molecular Biology of the Cell*. 19: 4177-4187.
- Liu, Y., Vidali, L. (2011). Efficient Polyethylene Glycol (PEG) Mediated Transformation of the Moss *Physcomitrella patens*. *J. Vis. Exp.* (50), e2560, DOI: 10.3791/2560.
- Menand, B., Calder, G., Dolan, L. (2007). Both chloronemal and caulonemal cells expand by tip growth in the moss *Physcomitrella patens*. *Journal of Experimental Biology*. 11: 633-675.
- Pashkova, N., Jin, Y., Ramaswamy, S., Weisman, L. (2006). Structural basis for myosin V discrimination between distinct cargoes. *The EMBO Journal*. 25: 693-700.
- Peremyslov, V., Mockler, T., Filichkin, S., Fox, S., Jaiswal, P., Makarova, K., Koonin, E., Dolja, V. (2011). Expression, Splicing, and Evolution of the Myosin Gene Family in Plants. *Plant Physiology*. 155: 1191-1204.

- Peremyslov, V., Prokhnevsky, A., Avisar, D., Dolja, V. (2008). Two Class XI Myosins Function in Organelle Trafficking and Root Hair Development in *Arabidopsis*. *Plant Physiology*. 146 (3): 1109-1116.
- Peremyslov, V., Prokhnevsky, A., Dolja, V. (2010). Class XI Myosins Are Required for Development, Cell Expansion, and F-Actin Organization in *Arabidopsis*. *The Plant Cell*. 22 (6): 1883-1897).
- Preuss, M., Serna, J., Falbel, T., Bednarek, S., Nielsen, E. (2004). The Arabidopsis Rab GTPase RabA4b Localizes to the Tips of Growing Root Hair Cells. *The Plant Cell*. 16: 1589-1603.
- Rensing, S., Lang, D. et al. (2008). The *Piscomitrella* Genome Reveals Evolutionary Insights into the Conquest of Land by Plants. *Science*. 319 (5859): 64-69.
- Saito, C. and Ueda, T. (2009). Functions of Rab and SNARE Proteins in Plant Life. *International Review of Cell and Molecular Biology*, 272: 183-233.
- Santiago-Tirado, F., Legesse-Miller, A., Schott, D., Bretscher, A. (2011). PI4P and Rab Inputs Collaborate in Myosin-V-Dependent Transport of Secretory Compartments in Yeast. *Developmental Cell*. 20: 47-59.
- Schott, D., Ho, J., Pruyne, D. and Bretscher, A. (1999). The COOH-Terminal Domain of Myo2p, a Yeast Myosin V, Has a Direct Role in Secretory Vesicle Targeting. *The Journal of Cell Biology*. 147(4): 791-807.
- Sparkes, Inogen A. (2010). Motoring around the plant cell: insights from plant myosins. *Biochemical Society Transactions*, 38: 833-838.
- Szumanski, A., and Nielsen, E. (2009). The Rab GTPase RabA4d Regulates Pollen Tube Tip Growth in *Arabidopsis thaliana*. *The Plant Cell*. 21: 526-544.

- Thole, J., Vermeer, J., Zhang, Y., Gadella, T., Nielsen, E. ROOT HAIR DEFECTIVE<sub>4</sub> Encodes a Phosphatidylinositol-4-Phosphate Phosphatase Required for Proper Root Hair Development in *Arabidopsis thaliana*. (2008). *The Plant Cell*. 20: 381-395.
- Tominaga M, Kojima H, Yokota E, Orii H, Nakamori R, Katayama E, Anson M, Shimmen T, Oiwa, K. (2003). Higher plant myosin XI moves processively on actin with 35 nm steps at high velocity. *EMBO J*. 22: 1263-1272.
- Vidali, L., Augustine, R., Kleinman, K., Bezanilla, M. (2007). Profilin Is Essential for Tip Growth in the Moss *Physcomitrella patens*. *The Plant Cell*. 19: 3705-3722.
- Vidali, L., Rounds, C., Hepler, P., Bezanilla, M. (2009a). Lifeact-mEGFP Reveals a Dynamic Apical F-Actin Network in Tip Growing Plant Cells. *PLoS ONE*. 4(5) e5744. Doi:10.1371/journal.pone.0005744.
- Vidali, L., van Gisbergen, P., Guérin, C., Franco, P., Li, M., Burkart, G., Augustine, R., Blanchion, L., Bezanilla, M. (2009b). Rapid formin-mediated actin-filament elongation is essential for polarized plant cell growth. *PNAS*. 106(32): 13341-13346.
- Vidali, L., Graham, B.M., Augustine, R.C., Kerdavid, E. Tüzel, E. and Magdalena Bezanilla. (2010). Myosin XI is Essential for Tip Growth in *Physcomitrella patens*. *The Plant Cell*, 22: 1868-1882.
- Yokota, E., Ueda, H., Hashimoto, K., Orii, H., Shimada, T., Hara-Nishimura, I., Shimmen, T. (2011). Myosin XI-Dependent Formation of Tubular Structures from Endoplasmic Reticulum Isolated from Tobacco Cultured BY-2 Cells. *Plant Physiology*. 156: 129-143.
- Žarský, V., Cvrčková, F., Potocký, M. and Hála, M. (2009). Exocytosis and cell polarity in plants- exocyst and recycling domains. *New Phytologist*, 183: 255-272.

Zhao, Y., Yan, A., Feijó, J., Furutani, M., Takenawa, T., Hwang, I., Fu, Y., Yang, Z. (2010).  
Phosphoinositides Regulate Clathrin-Dependant Endocytosis at the Tip of Pollen Tubes  
in *Arabidopsis* and Tobacco. *The Plant Cell*. 22(12): 4031-4044.